Research Article | Vol. 25, No. 10 | 15 May 2017 | OPTICS EXPRESS 10743
Optics EXPRESS

Optimization in nanocoated D-shaped optical fiber sensors

IGNACIO DEL VILLAR,[1,*] PABLO ZUBIATE,[2] CARLOS R. ZAMARREÑO,[1] FRANCISCO J. ARREGUI,[1,2] AND IGNACIO R. MATIAS[1]

[1]*Institute of Smart Cities (ISC), Public University of Navarra, 31006 Pamplona, Spain*
[2]*Electrical and Electronic Engineering Department, Public University of Navarra, 31006 Pamplona, Spain*
**ignacio.delvillar@unavarra.es*

Abstract: Nanocoated D-shaped optical fibers have been proven as effective sensors. Here, we show that the full width at half minimum (FWHM) of lossy mode resonance can be reduced by optimizing the nanocoating width, thickness and refractive index. As a counterpart, several resonances are observed in the optical spectrum for specific conditions. These resonances are caused by multiple modes guided in the nanocoating. By optimizing the width of the coating and the imaginary part of its refractive index, it is possible to isolate one of these resonances, which allows one to reduce the full width at half minimum of the device and, hence, to increase the figure of merit. Moreover, it is even possible to avoid the need of a polarizer by designing a device where the resonance bands for TE and TM polarization are centered at the same wavelength. This is interesting for the development of optical filters and sensors with a high figure of merit.

OCIS codes: (060.2370) Fiber optics sensors; (310.0310) Thin films; (230.7370) Waveguides.

References and links

1. T. Allsop, R. Neal, C. Mou, K. Kalli, S. Saied, S. Rehman, D. J. Webb, P. Culverhouse, J. L. Sullivan, and I. Bennion, "Formation and characterisation of ultra-sensitive surface plasmon resonance sensor based upon a nano-scale corrugated multi- layered coated D-shaped optical fibre," IEEE J. Quantum Electron. **48**(3), 1–19 (2012).
2. A. Patnaik, K. Senthilnathan, and R. Jha, "Graphene-Based Conducting Metal Oxide Coated D-Shaped Optical Fiber SPR Sensor," IEEE Photonics Technol. Lett. **27**(23), 2437–2440 (2015).
3. A. Andreev, B. Pantchev, P. Danesh, B. Zafirova, E. Karakoleva, E. Vlaikova, and E. Alipieva, "A refractometric sensor using index-sensitive mode resonance between single-mode fiber and thin film amorphous silicon waveguide," Sens. Actuators B Chem. **106**(1), 484–488 (2005).
4. A. T. Andreev, B. S. Zafirova, E. I. Karakoleva, A. O. Dikovska, and P. A. Atanasov, "Highly sensitive refractometers based on a side-polished single-mode fibre coupled with a metal oxide thin-film planar waveguide," J. Opt. A, Pure Appl. Opt. **10**(3), 035303 (2008).
5. P. Zubiate, C. R. Zamarreño, I. Del Villar, I. R. Matias, and F. J. Arregui, "High sensitive refractometers based on lossy mode resonances (LMRs) supported by ITO coated D-shaped optical fibers," Opt. Express **23**(6), 8045–8050 (2015).
6. P. Zubiate, C. R. Zamarreno, I. Del Villar, I. R. Matias, and F. J. Arregui, "Experimental study and sensing applications of polarization-dependent lossy mode resonances generated by D-shape coated optical fibers," J. Lightwave Technol. **33**(12), 2412–2418 (2015).
7. F. J. Arregui, I. Del Villar, C. R. Zamarreño, P. Zubiate, and I. R. Matias, "Giant sensitivity of optical fiber sensors by means of lossy mode resonance," Sens. Actuators B Chem. **232**, 660–665 (2016).
8. F. Yang and J. R. Sambles, "Determination of the optical permittivity and thickness of absorbing films using long range modes," J. Mod. Opt. **44**(6), 1155–1164 (1997).
9. I. Del Villar, M. Hernaez, C. R. Zamarreño, P. Sánchez, C. Fernández-Valdivielso, F. J. Arregui, and I. R. Matias, "Design rules for lossy mode resonance based sensors," Appl. Opt. **51**(19), 4298–4307 (2012).
10. B. D. Gupta, S. K. Srivastava, and R. Verma, *Fiber Optic Sensors Based on Plasmonics* (World Scientific Publishing Co, 2015).
11. I. Del Villar, A. B. Socorro, M. Hernaez, J. M. Corres, C. R. Zamarreño, P. Sanchez, F. J. Arregui, and I. R. Matias, "Sensors based on thin-film coated cladding removed multimode optical fiber and single-mode multimode single-mode fiber : a comparative study," J. Sens. **763762**, 1–7 (2015).
12. A. B. Socorro, I. Del Villar, J. M. Corres, F. J. Arregui, and I. R. Matias, "Spectral width reduction in lossy mode resonance-based sensors by means of tapered optical fibre structures," Sens. Actuators B Chem. **200**, 53–

#283235 https://doi.org/10.1364/OE.25.010743
Journal © 2017 Received 23 Mar 2017; revised 21 Apr 2017; accepted 24 Apr 2017; published 2 May 2017

Optics EXPRESS

60 (2014).
13. I. Del Villar, C. R. Zamarreño, M. Hernaez, F. J. Arregui, and I. R. Matias, "Lossy mode resonance generation with indium-tin-oxide-coated optical fibers for sensing applications," J. Lightwave Technol. **28**(1), 111–117 (2010).
14. I. Del Villar, F. J. Arregui, I. R. Matias, A. Cusano, D. Paladino, and A. Cutolo, "Fringe generation with non-uniformly coated long-period fiber gratings," Opt. Express **15**, 1373–1378 (2007).
15. I. H. Malitson, "Interspecimen comparison of the refractive index of fused silica," J. Opt. Soc. Am. **55**(10), 1205–1209 (1965).
16. G. M. Hale and M. R. Querry, "Optical constants of water in the 200-nm to 200-microm wavelength region," Appl. Opt. **12**(3), 555–563 (1973).
17. F. Chiavaioli, P. Biswas, C. Trono, S. Bandyopadhyay, A. Giannetti, and S. Tombelli, "Biosensors and Bioelectronics Towards sensitive label-free immunosensing by means of turn-around point long period fi ber gratings," Biosens. Bioelectron. **60**, 305–310 (2014).
18. G. Quero, M. Consales, R. Severino, P. Vaiano, A. Boniello, A. Sandomenico, M. Ruvo, A. Borriello, L. Diodato, S. Zuppolini, M. Giordano, I. C. Nettore, C. Mazzarella, A. Colao, P. E. Macchia, F. Santorelli, A. Cutolo, and A. Cusano, "Long period fiber grating nano-optrode for cancer biomarker detection," Biosens. Bioelectron. **80**, 590–600 (2016).
19. J. Goicoechea, C. R. Zamarreño, I. R. Matias, and F. J. Arregui, "Utilization of white light interferometry in pH sensing applications by mean of the fabrication of nanostructured cavities," Sens. Actuators B Chem. **138**(2), 613–618 (2009).
20. I. Del Villar, F. J. Arregui, C. R. Zamarreño, J. M. Corres, C. Bariain, J. Goicoechea, C. Elosua, M. Hernaez, P. J. Rivero, A. B. Socorro, A. Urrutia, P. Sanchez, P. Zubiate, D. Lopez, N. De Acha, J. Ascorbe, and I. R. Matias, "Optical sensors based on lossy-mode resonances," Sens. Actuators B Chem. **240**, 174–185 (2017).
21. M. Marciniak, J. Grzegorzewski, and M. Szustakowski, "Analysis of lossy mode cut-off conditions in planar waveguides with semiconductor guiding layer," IEE Proc., J Optoelectron. **140**(4), 247–252 (1993).
22. M. Lohmeyer, N. Bahlmann, O. Zhuromskyy, H. Dötsch, and P. Hertel, "Phase-matched rectangular magnetooptic waveguides for applications in integrated optics isolators: numerical assessment," Opt. Commun. **158**(1-6), 189–200 (1998).
23. A. Shalabney and I. Abdulhalim, "Figure-of-merit enhancement of surface plasmon resonance sensors in the spectral interrogation," Opt. Lett. **37**(7), 1175–1177 (2012).

1. Introduction

Nanocoated D-shaped optical fibers have great potential in the domain of sensors. Two main groups can be distinguished: surface plasmon resonance (SPR)- [1,2], and lossy-mode resonance (LMR)-based devices [3–7]. Regarding the latter group, some researchers classify LMR as guided mode resonance [8] or transverse electric (TE) and transverse magnetic (TM) resonances [3]. However, in order to avoid confusion, a single notation (LMR) will be used throughout this work.

LMR-based optical fiber sensors have interesting properties: it is possible to position the resonance at a specific wavelength simply by controlling the coating thickness. Furthermore, the resonance can be generated both for TE and TM polarization. In addition, LMRs can be obtained under the condition that the real part of the nanocoating permittivity is positive and higher in magnitude than both its own imaginary part and that of the material surrounding the nanocoating. Consequently, a wide range of materials satisfies this condition, such as metallic oxides and polymers. Moreover, multiple resonances in the optical spectrum can be obtained [9].

In the first publications on LMR based nanocoated D-shaped fibers, sensitivities of the order of 3000–8000 nm per refractive index unit (nm/RIU) in the water refractive index region were attained [3–6]. However, in a recent publication, a record sensitivity of 15000 nm/RIU was obtained in the water region and another record of 300000 nm/RIU in the proximities of the silica refractive index, which certifies that the device can compete with the best refractometric optical sensors [7]. In this last work, the focus was centered on the achievement of high sensitivities. Now that the good performance of this photonic device has been demonstrated, the aim is to improve the figure of merit (i.e. the ratio between sensitivity and full-width at half minimum- FWHM), which is a typical quality parameter for SPR sensors [10].

It is well known that the sensitivity is increased by selecting the first LMR [9]. However, the first LMR shows the broadest resonance [11], which prevents the figure of merit from

Optics EXPRESS

being improved. A good method for reducing the width of the resonance is to use a nanocoated tapered single-mode fiber. With this device, there is a coupling of light transmitted through a single mode in the optical fiber core to the nanocoating, which allows the dispersion caused by coupling of light transmitted through multiple modes in the core to nanocoating to be reduced [12].

A step forward was attained with the D-shaped single mode fiber. Unlike cylindrically symmetrical devices, where the LMR may be composed of the combined coupling with TE and TM polarization [13], D-shaped fibers allow one to separate between TE and TM polarizations, as well as to reduce the resonance width [5]. In addition, light transmitted through a D-shaped single-mode fiber combines the resonance width reduction obtained with nanocoated tapered single-mode fibers (thanks to the coupling of light transmitted through a single mode present in the core to the nanocoating), with the separation of the TE and TM polarization contributions.

However, the resonance width can be further greatly reduced by taking into account some additional considerations analyzed here. A first way, which is proved numerically and experimentally in this work, is to increase the nanocoating real part of the refractive index. Controlling the imaginary part is a more difficult task. Consequently, this parameter has been mainly analyzed theoretically. By analyzing the imaginary part it is possible to obtain multiple sharp resonance bands. This occurs because in the D-shaped optical fiber multiple modes are guided in the nanocoating instead of one for each LMR. A further numerical analysis has been performed on isolating the contribution of each of these modes, which permits to control the width of the resonance. Moreover, through the adequate selection of the dimensions of the nanocoating, it is even possible to fit both resonances obtained for TE and TM at the same wavelength, which avoids using a polarizer. Though the physical implementation of such devices is difficult, with the evolution of nanotechnology in the next years this could become a reality and high quality factor sensors could be developed.

2. Materials and Methods

The sensing setup is depicted in Fig. 1(a): light from a broadband source is transmitted through the optical structure and collected in an optical spectrum analyzer.

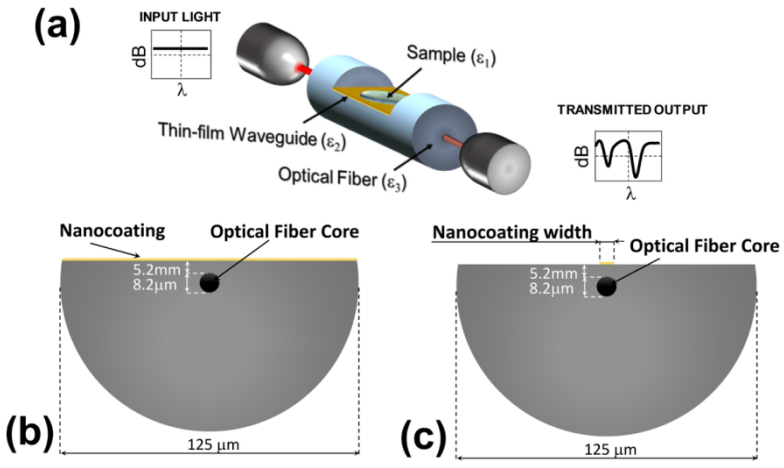

Fig. 1. (a) Sensing setup: a broadband source launches light into a nanocoated D-shaped fiber and light is monitored in an optical spectrum analyzer. (b) Transverse section of D-shaped fiber coated with a nanocoating that covers the entire waveguide width. (c) Transverse section D-shaped fiber coated with a nanocoating with a limited width.

Two types of structures where analyzed: one where the transverse section of the D-shaped fiber was coated with a coating that covers the entire waveguide [Fig. 1(b)], and another

Optics EXPRESS

where the transverse section of the D-shaped fiber was coated with a thin-film that that is limited in width [Fig. 1(c)]. Laser micromachining could be a possible way to obtain this setup experimentally [14].

For the numerical analysis of both structures, FIMMWAVE® was used. The propagation was obtained with FIMMPROP, a module integrated with FIMMWAVE. Three sections were defined: a single-mode fiber (SMF) segment, a side polished SMF segment and another SMF segment. For the SMF segment, the finite difference method (FDM) was used, because it is the most accurate method available for a cylindrical waveguide, whereas for the side polished SMF segment, with a more complex profile, the finite-element method (FEM) Solver was used. One mode was analyzed in the SMF section because light is guided through the core, whereas in the side polished SMF 100 modes were analyzed towards a convergence in the results.

A standard single mode fiber Corning® SMF-28 with a side-polished length of 1.7 cm was used. The refractive index of the optical fiber cladding, made of fused silica, was estimated with the Sellmeier equation:

$$n^2(\omega) = 1 + \sum_{j=1}^{m} \frac{B_j \omega_j^2}{\omega_j^2 - \omega^2} \tag{1}$$

with parameters: B_1=0.691663, B_2=0.4079426, B_3=0.8974794, λ_1=0.0684043 μm, λ_2= 0.1162414, and λ_3= 9.896161, where $\lambda_j = 2\pi c/\omega_j$ and c is the speed of light in a vacuum [15]. The optical fiber core refractive index for the simulations was obtained, according to the specifications from Corning®, by increasing the refractive index of the cladding by 0.36%.

The surrounding medium refractive index was set to 1.321, the refractive index of water at 1400 nm, the central wavelength of the resonance in Fig. 2 [16]. The analysis will be focused on this index because it is the region where the performance of chemical and biological sensors can be compared [17,18], and this type of sensors have a great interest nowadays.

Two different coatings were analyzed. The first one was a high refractive index material: indium tin oxide (ITO). A 92 nm coating of indium tin oxide (ITO) was deposited with DC sputtering (pressure of argon of 9×10^{-2} mbar and current intensity applied to the ITO target 150 mA). Its refractive index ranges from 1.93+0.007i to 1.9+0.02i in the wavelength range 1150–1700 nm [7].

The second material was PAH/PAA, a combination of two polymers deposited with a layer-by-layer technique: poly(allylamine hydrochloride) (PAH) and poly(acrylic acid) (PAA). In order to deposit this nanocoating, the D-shaped optical fiber was immersed in 1 M KOH for 10 minutes, followed by washing in ultrapure water in order to acquire a prior negative charge. The fabrication process consisted of the alternate immersion of the substrate into two solutions of PAH (10 mM concentration and adjusted to pH 4.0) and PAA (10 mM concentration and adjusted to pH 4.0). The optical fiber device was immersed in the PAH solution and the PAA solution for 2 minutes each. The fiber was rinsed repeatedly in ultrapure water between these two immersion steps. The structure obtained after this process is known as a layer pair, and the procedure was repeated until the required thickness was obtained. Here, 63 layer pairs were deposited. The refractive index used in the numerical analysis was 1.475+0.001i [9], and a total thickness of 1110 nm (17.6 nm/per layer pair) was set to fit the position of the resonance with the experimental results. This value was very close to that obtained in [19].

Both ITO and PAH/PAA permit to generate LMRs, which can be obtained with both transverse electric (TE) and transverse magnetic (TM) polarized light. Indeed, the performance with both resonances is similar. However, for the sake of simplicity, and in order to see the difference with SPRs (SPRs are obtained with just TM polarization), only TE polarization will be analyzed. However, in the final section, where the purpose is to obtain a design where a polarizer is not needed, we will analyze the position of both TE and TM resonances.

Optics EXPRESS

3. Results and discussion

Figure 2 shows the numerical and experimental spectra obtained with D-shaped fibers coated both with PAH/PAA and ITO for the parameters indicated in section 2. With both PAH/PAA and ITO coatings, a resonance centered at approximately 1400 nm is obtained (the position of the resonance can be easily tuned anywhere in the optical spectrum by changing the nanocoating thickness [9]). It can be observed that with PAH/PAA the resonance is wider than with ITO. Moreover, it is well known that lossy mode resonances are more sensitive if the refractive index is higher [9,20]. In view that the figure of merit is the ratio between sensitivity and full-width at half minimum it is obvious that the best option towards a figure of merit enhancement is an ITO coated D-shaped fiber. The not perfectly smooth shape in the experimental spectra is due to inaccuracies in the deposition of the nanocoating. The deposition of the D-shaped fiber is performed in such a way that it is not possible to rotate the platform where the fiber is rotated while the deposition is being performed.

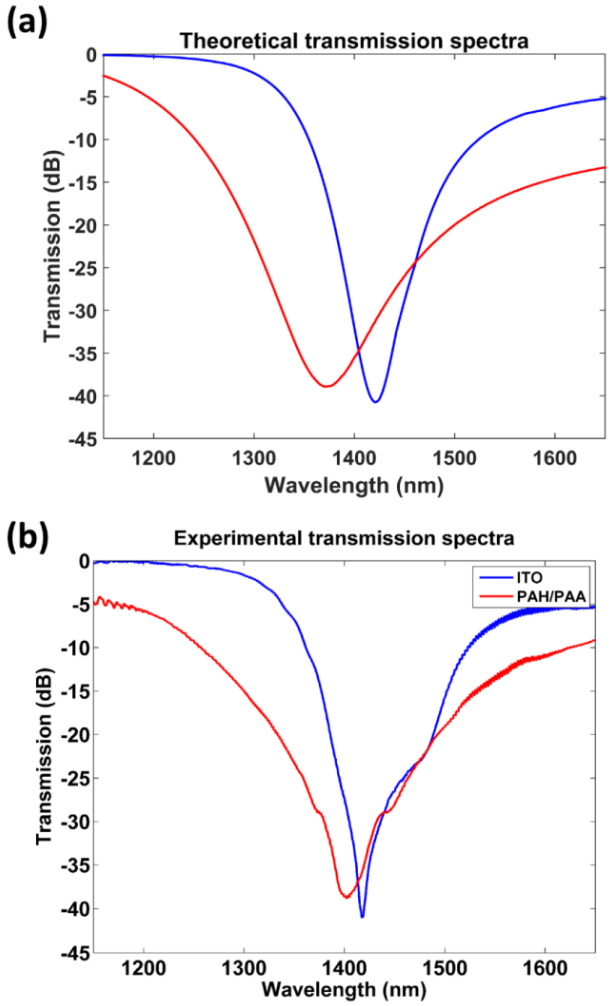

Fig. 2. Transmission spectrum for TE polarization lossy mode resonance. (a) Numerical results with both ITO and polymer PAH/PAA. (b) Experimental results with both ITO and polymer PAH/PAA.

Optics EXPRESS

Lossy mode resonances are generated if a mode guided in the optical fiber experiences a transition to guidance in the thin-film [13]. However, if we contrast the theoretical spectrum of the ITO coated D-shaped fiber in Fig. 2 with the real part of the effective index of modes guided through this structure in Fig. 3, 27 modes experience a transition to guidance in the thin-film, instead of one, as it is the case in cylindrically symmetric structures [20].

In order to better understand this phenomenon, the electric field intensity in the transverse section at a wavelength of 1350 nm is analyzed in Fig. 4. This wavelength permits to observe modes guided in the nanocoating and non-guided modes in the nanocoating as well.

We present the first 15 modes. Modes 1–7 and 9–12 are those guided in the nanocoating, mode 8 is the core mode, and modes 13–15 are the cladding modes. The fact that the nanocoating is a rectangle (finite in width and in height) and not an annulus (finite in radial axis but not in azimuthal axis) causes the presence of several transitions, corresponding to the guidance of different modes; whereas in the cladding removed coated optical fiber annulus, only one mode is guided in each LMR. Even though, there is a single resonance in Fig. 2. Consequently, the guidance of multiple modes apparently plays no role in the results.

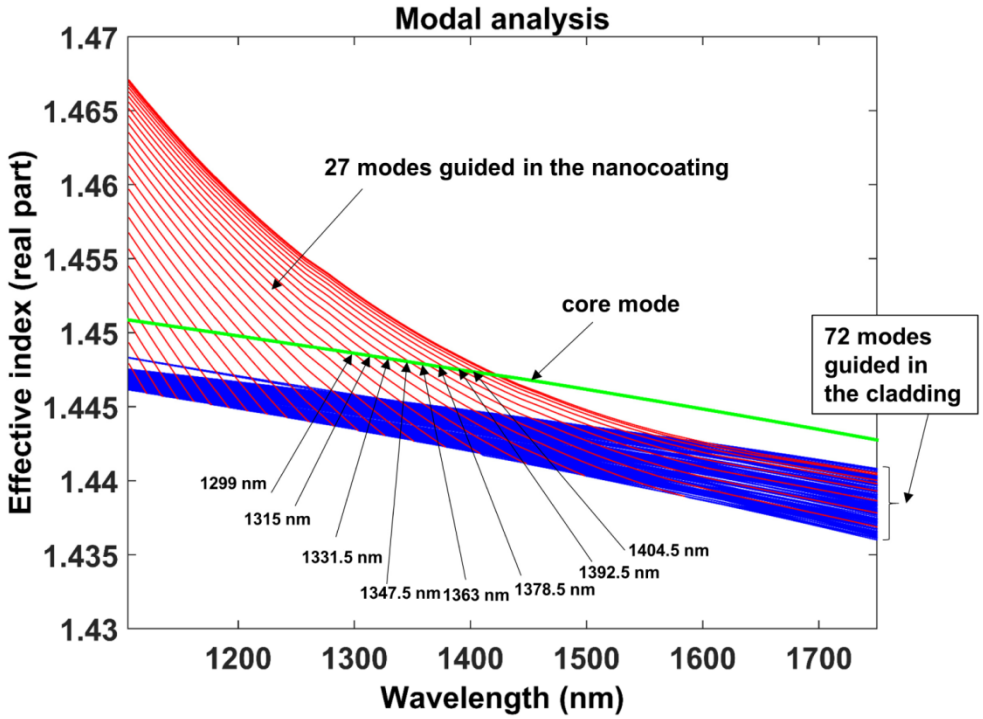

Fig. 3. Real part of the effective indices of the first 100 modes guided in an ITO nanocoated D-shaped fiber (core mode in green, modes guided in the nanocoating in red and cladding modes in blue). They correspond with the modes used for the theoretical spectrum in Fig. 2(a).

Optics EXPRESS

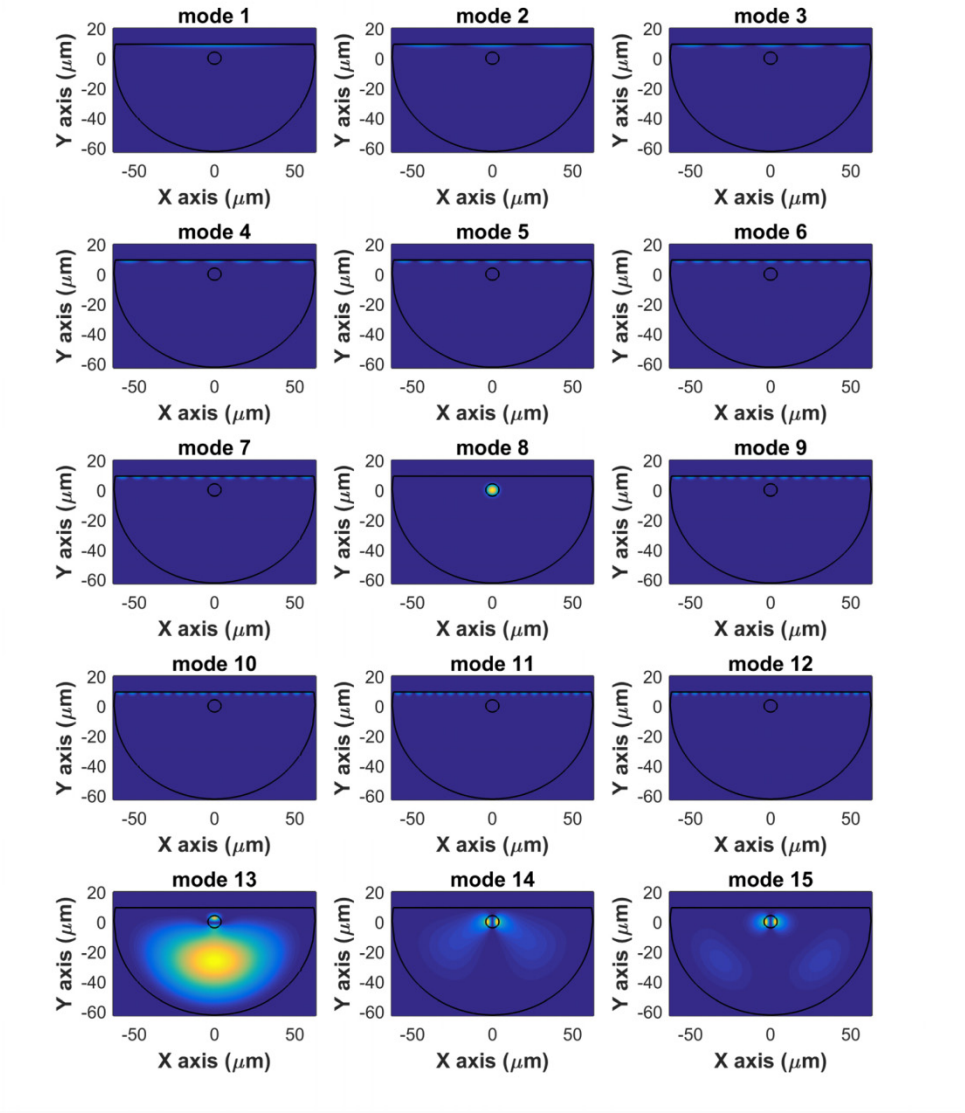

Fig. 4. Electric field intensity of modes. Intensity of first 15 modes in the transverse section of the ITO coated D-shaped fiber (the structure is like that represented in Fig. 1(b), with a nanocoating that covers the entire waveguide). The center is the fiber core. Above the center, in the nanocoating, the different lossy modes can be observed (modes 1–7 and 9–12).

However, by analyzing the evolution of the transmission spectrum as a function of the imaginary part of the refractive index, it will be verified that this parameter also allows seeing the effect of the guidance of several modes. In order to simplify the analysis, a constant imaginary part as a function of wavelength has been assumed in each case. The selected values are: 0.0001, 0.0005, 0.001, 0.002, 0.004 and 0.008. For the sake of comparison, also the theoretical spectrum obtained in Fig. 2(a) is plotted. The ITO model used for this last theoretical spectrum was based on ellipsometric measurements and it presented an imaginary part 0.013 at 1410 nm [7], the center of the LMR, which is higher than the rest of values analyzed.

Optics EXPRESS

Two stages can be observed in Fig. 5. In the first one, there is a progressive increase of the depth of the attenuation band with several marked resonances at the wavelengths where the mode transitions to guidance in the nanocoating occur. Indeed there is correspondence between the positions of these bands with the wavelengths where the modes start to exceed the effective index of the core mode, a point that is related to the phase matching condition of each nanocoating mode with the core mode (the phase matching condition is the point where the core mode effective index and the mode guided in the nanocoating present the same real part of the propagation constant and their modal fields considerably overlap) [21]. After a maximum (imaginary part 0.004), the LMR broadens, and its depth starts to decrease at the same time as the marked peaks disappear. This is because one property of LMRs is to broaden as well as the imaginary part increases [9,20]. Consequently, each LMR overlaps each other and the spectrum is smoothed.

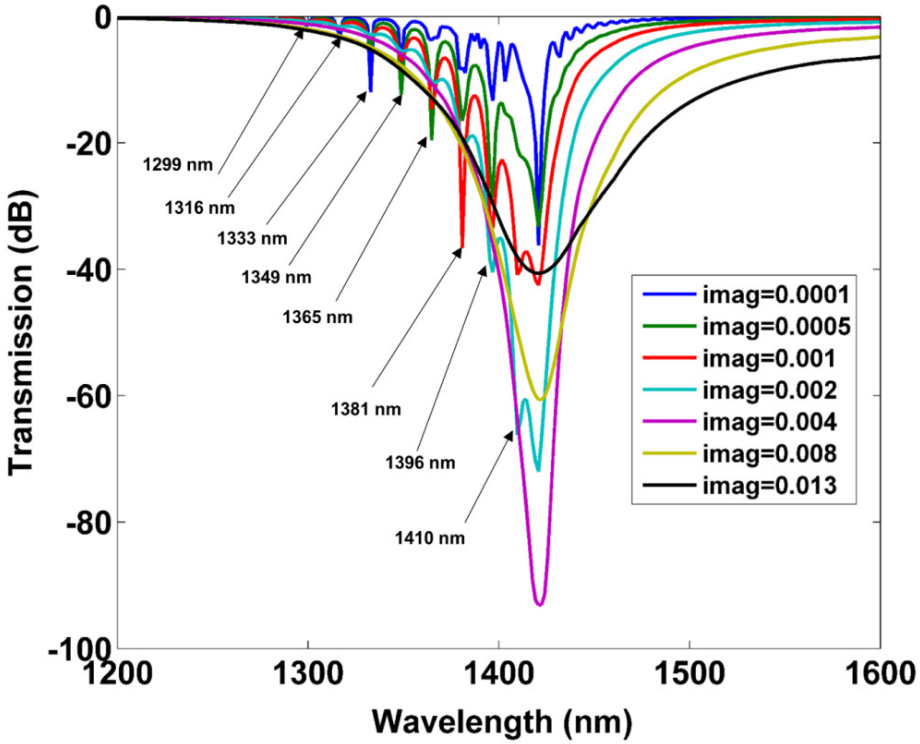

Fig. 5. Transmission spectra for TE polarization lossy mode resonance. Different imaginary part refractive indices have been analyzed: 0.0001, 0.0005, 0.001, 0.002, 0.004, 0.008 and the refractive index of ITO deposited with DC sputtering (0.013 at wavelength 1410 nm – see section 2).

As an example of an experimental presence of marked resonances like those observed in Fig. 5, in Fig. 6 we show the optical spectrum of another ITO coated D-shaped fiber. Depending on the conditions of the sputtering deposition there are small changes in the refractive index of the coating and in this case the resonances of Fig. 5 are visible.

Optics EXPRESS

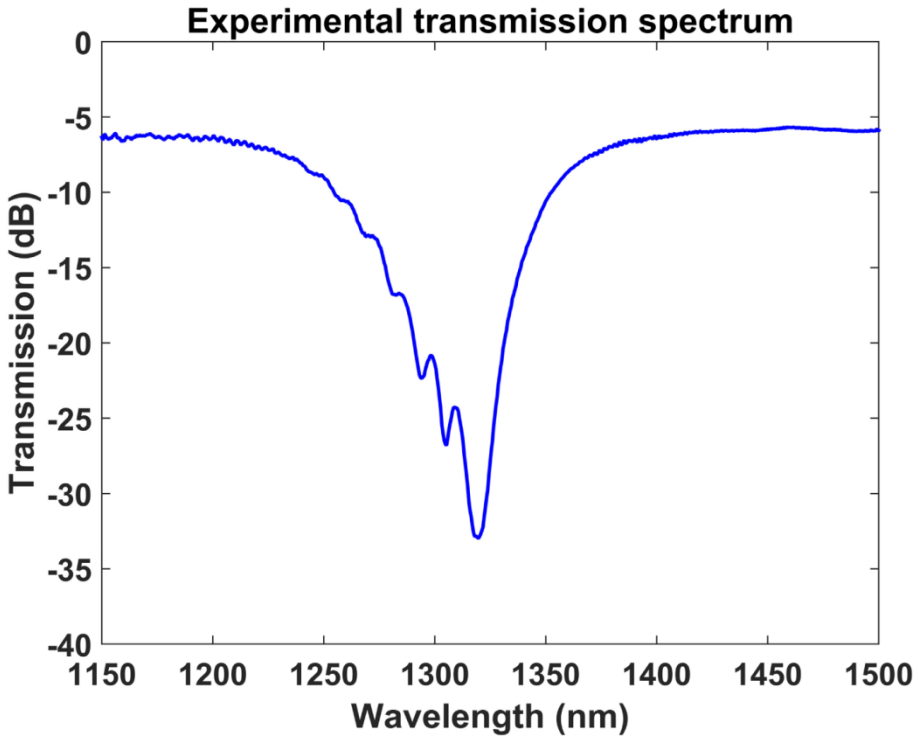

Fig. 6. Transmission spectrum in an ITO coated D-shaped optical fiber with presence of small resonances belonging to the guidance of different modes in the nanocoating.

The next step will be to isolate one of the bands in Fig. 5. To this end, the case with the deepest and narrowest resonance will be selected, which corresponds to an imaginary part of the nanocoating refractive index 0.004. The FWHM for this nanocoating refractive index is 24.8 nm, whereas the figure of merit is 4540/24.8=183.1RIU^{-1} (4540 is the sensitivity of the device in nm/RIU in the water refractive index region, calculated by analyzing the wavelength shift when surrounding refractive index changes from 1.321 to 1.331). On the other hand, the figure of merit for a coating with an imaginary part 0.004 is 4540/6.4= 709.4 RIU^{-1} (the increase is due to the decrease in the FWHM). Due to this, we will continue our analysis, henceforward, for a value 0.004 in the imaginary part of the ITO nanocoating.

Considering that the spectra in Fig. 5 present a several minima, we will analyze the effect of reducing the width of the nanocoating while maintaining its thickness. In Fig. 7, the spectrum and real part of the effective index of modes are represented for four different nanocoating widths: 5, 10, 20 and 30 μm. It is obvious that fewer modes are guided as the width is reduced (see Fig. 8), which allows us to obtain one single band for 5 and 10 μm (see Fig. 7). In fact, for a width of 10 μm, two modes are guided; but one of them is too far separated from the LMR and plays no role in the spectral range under analysis. It is interesting to see that the case with a width of 10 μm shows a FWHM of 3.3 nm, which improves the result obtained without coating width reduction for the same refractive index by a factor of two. However, the same improvement is not observed in the figure of merit because, due to the width reduction, there is an influence of the surrounding medium refractive index above and at both sides of the coating, which leads to the lower sensitivity of 3770 nm/RIU in the water refractive index region. Nevertheless, the figure of merit is increased: 3770/3.3= 1021.2 RIU^{-1}.

Optics EXPRESS

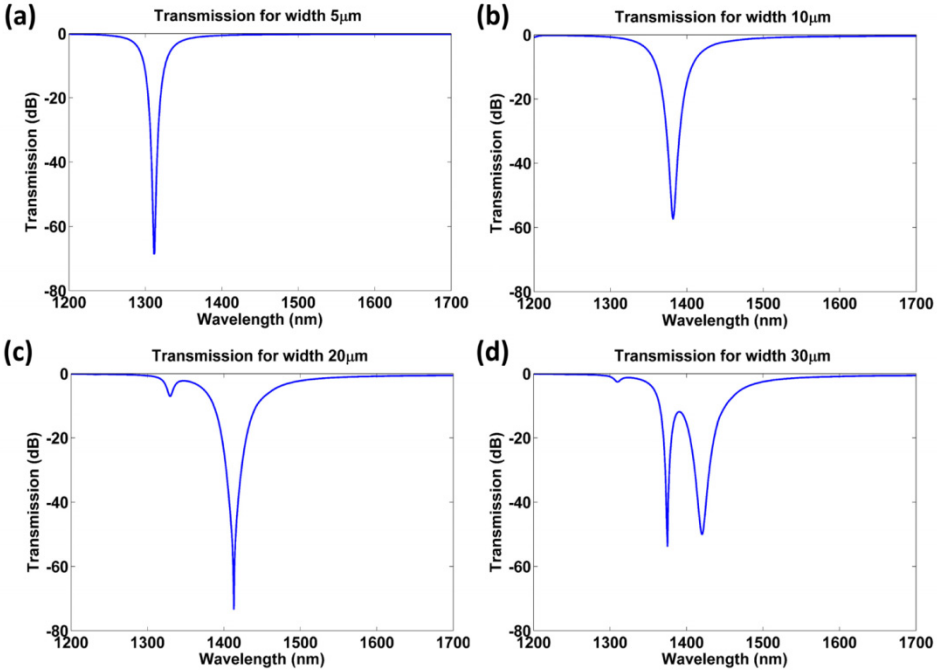

Fig. 7. Transmission spectrum in 92 nm-thick ITO coated D-shaped optical fiber. Four different coating widths have been analyzed: (a) 5 μm, (b) 10 μm, (c) 20 μm and (d) 30 μm.

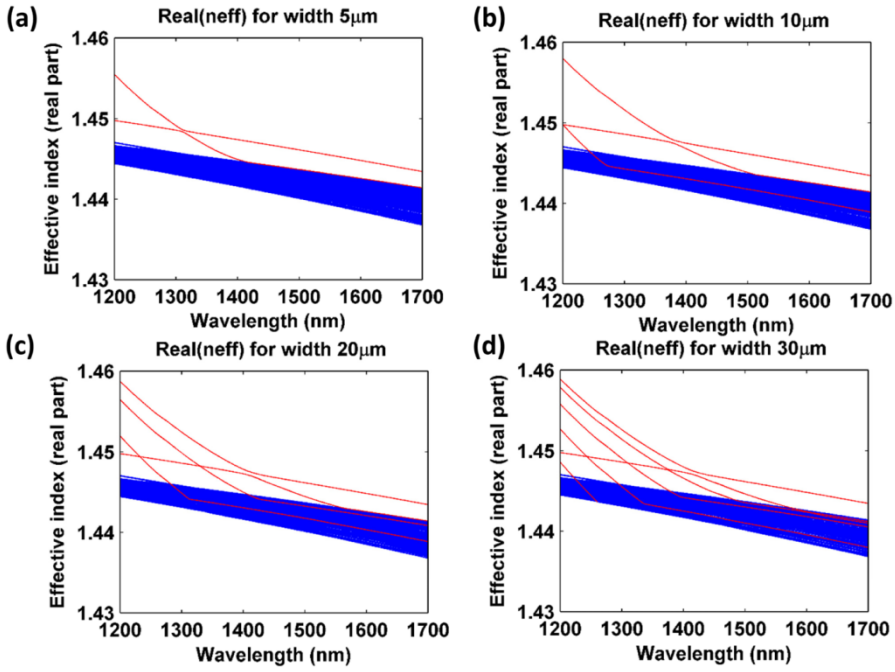

Fig. 8. Effective index of first 100 modes in 92 nm-thick ITO coated D-shaped optical fiber. Four different coating widths have been analyzed: (a) 5 μm, (b) 10 μm, (c) 20 μm and (d) 30 μm.

Optics EXPRESS

Another conclusion that can be extracted from Fig. 7 by comparing the results obtained for 5 μm and 10 μm is that the resonance is blue-shifted if the width is reduced. This is because the width starts to be lower than the core diameter. Consequently, the core mode is influenced by a finite-width nanocoating.

If we further reduce the coating width, a limit will be reached where the width is equal to the thickness. In other words, the section of the nanocoating is square. This situation is interesting as it should lead to another situation where the propagation of light is independent of the polarization of the light. In Fig. 9, different cases are analyzed. For a square of side 92 nm, it is not possible to observe any resonance in the wavelength range 1100–1600 nm. It is necessary to increase the side by up to 375 nm. For a fixed thickness of 375 nm, four different widths are analyzed: 375, 400, 425 and 450 nm.

It is evident that at 425 nm, the point where both polarizations match is found. This can be explained as the ITO layer is a planar-like raised strip waveguide on the silica substrate. According to Lohmeyer [22], in a thin and wide core, the propagation constant of the fundamental TE mode exceeds that of the fundamental TM mode. However, the device becomes a planar-like waveguide again if the rib is continuously narrowed and raised, but with the role of the transverse axes exchanged. Consequently, there is an intermediate configuration with an almost square core, where the modes match in wavelength (in the case of the ITO coated D-shaped fiber for 425×375 nm).

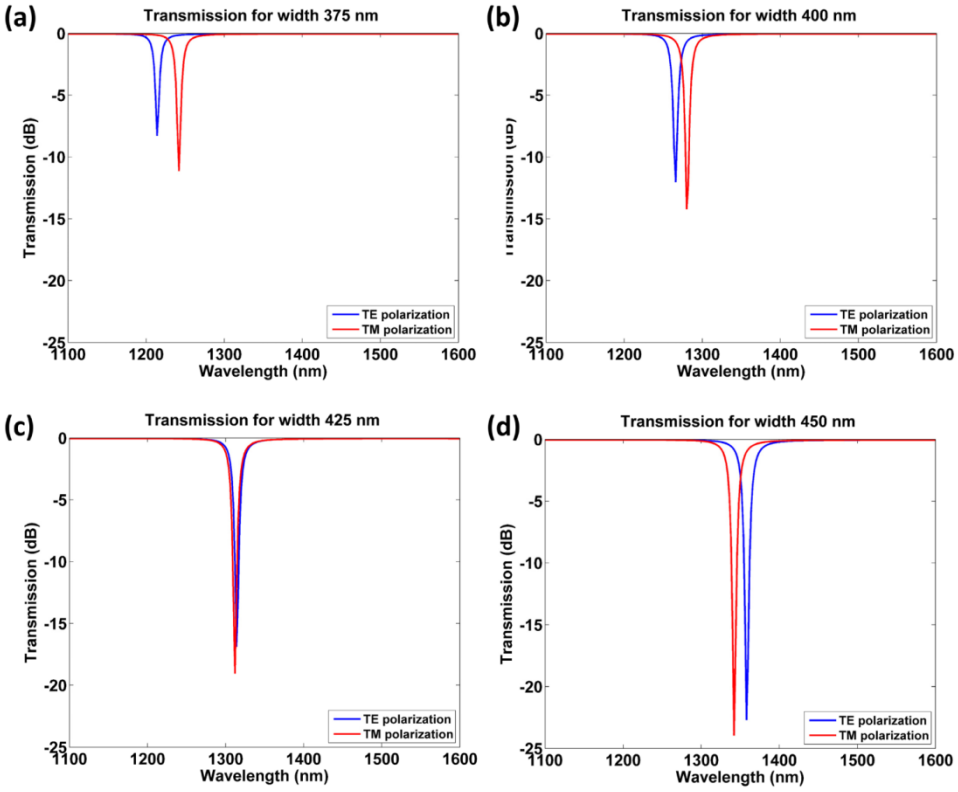

Fig. 9. Transmission spectrum for 375 nm thick ITO-coated D-shaped optical fiber. Four different coating widths have been analyzed under TE and TM polarization: (a) 375 nm, (b) 400 nm, (c) 425 nm and (d) 450 nm.

With this design the sensitivity is only 1760 nm/RIU due to the narrow width of the nanocoating (the narrow ITO thin-film has a lower effect on the core than a wider thin-film). As a result, the figure of merit is only 1760/2=830 RIU^{-1}. Even though this value is lower

Optics EXPRESS

than that obtained with the previous design, it is remarkable to say that the need for polarized light is avoided, which is quite interesting to obtain a simple and integrated nanocoated D-shaped fiber sensor. Moreover, the performance of this device is close to optimized surface plasmon resonance sensors analyzed in [21]. In that work the sensors were characterized with the ratio between the sensitivity and the full width at half maximum, a parameter considered by other authors as the figure of merit. The maximum value obtained was 200 RIU^{-1} [23], whereas the ratio between the sensitivity and the full width at half maximum for the design of Fig. 9(c) is 1760/8.3= 128 RIU^{-1}.

Table 1 presents a summary of the parameters of the configurations with ITO coatings analyzed here. The main conclusion is that a high increase in the figure of merit is obtained when optimizing the imaginary part of the nanocoating refractive index. A further increase is attained by reducing the nanocoating width, whereas a small reduction is caused by optimizing the structure towards a device independent of the polarization.

Table 1. ITO nanocoated D-shaped fiber parameters and the FWHM.

Nanocoating width	Nanocoating thickness	Nanocoating imaginary part	Full width at half maximum (FWHM)	Figure of Merit (FOM)	Polarization independent
123.5 µm	92 nm	0.007-0.02	24.8 nm	183.1 RIU^{-1}	No
123.5 µm	92 nm	0.004	6.4 nm	709.4 RIU^{-1}	No
10 µm	92 nm	0.004	3.3 nm	1021.2 RIU^{-1}	No
425 nm	375 nm	0.004	2 nm	830 RIU^{-1}	Yes

In order to prove the ability of this sensor to detect refractive index changes, a refractive index sweep in the range 1.3 to 1.335 was performed. In Fig. 10 the average value between the spectrum obtained at TE polarization and the spectrum obtained at TM polarization is shown for several refractive indices. A double peak is visible in the extreme cases, whereas in the center of Fig. 10 only one peak is distinguishable. The explanation can be found in Fig. 11, where the central wavelength for TE and TM polarization is represented as a function of the surrounding refractive index. The plots for both polarizations cross at 1.305, whereas out of this point there is a progressive separation between the values obtained for both polarizations.

In Fig. 11 also the minimum wavelength of the average value between TE and TM polarization is plotted (TE+TM). In the range from 1.3 and 1.32 the values obtained are the average values between those calculated for TE and TM polarization. However, above 1.32, as the bands split, the values approach either the TM case, because one of the two minima presents a lower value and the algorithm is based on tracking the wavelength with a minimum transmission. However, by using a simple algorithm (TE+TM polarization with processing), based on calculating the average between the shortest and the longest wavelengths that exceeds a specific attenuation value (i.e. −5 dB), it is possible to obtain values that represent the middle value between the wavelengths obtained for both TE and TM polarization. The sensitivity obtained in the range 1.3 to 1.335 is 1566 nm/refractive index unit.

Optics EXPRESS

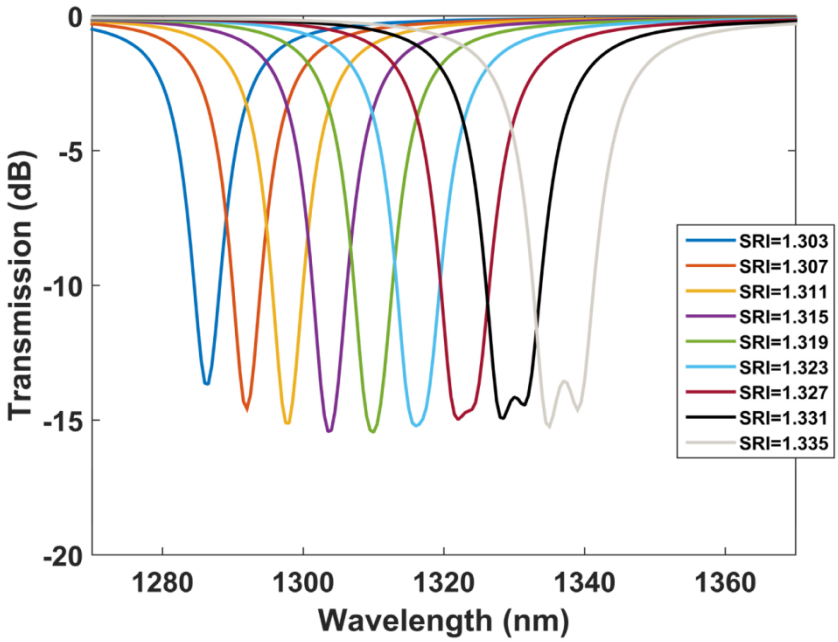

Fig. 10. Transmission spectra for different surrounding refractive indices (SRI) in a D-shaped fiber coated with a 425×375 nm ITO coating. The average value between TE and TM polarized transmission spectra has been computed. For high refractive indices the separation between TE and TM band is higher and two minima can be observed.

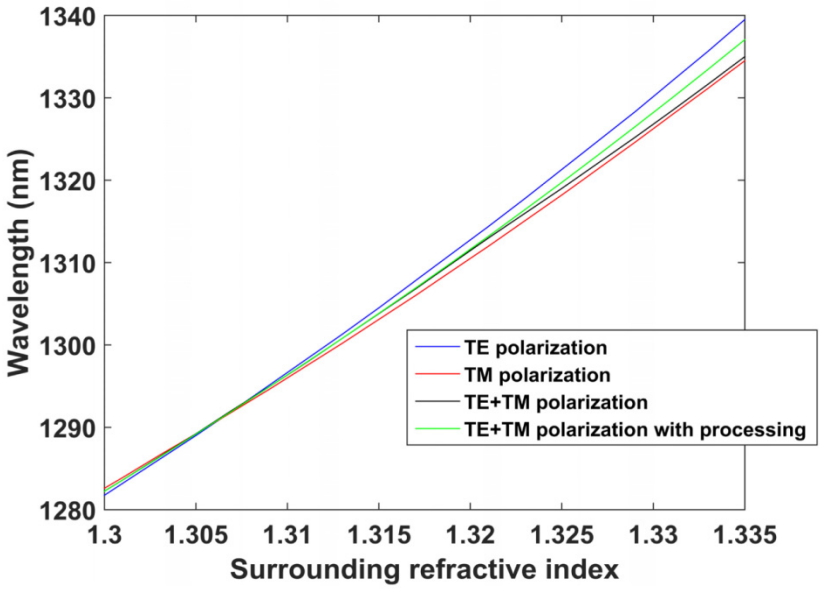

Fig. 11. Resonance wavelength versus surrounding refractive index (SRI) in a D-shaped fiber coated with a 425×375 nm ITO coating. Four cases have been analyzed: TE, TM, the average value between TE and TM, and the average value between TE and TM with an additional processing.

Optics EXPRESS

4. Conclusions

Contrary to cylindrically symmetrical structures, such as nanocoated cladding removed multimode fiber or tapered single mode fiber, where the transition to guidance of a mode of the optical fiber in the nanocoating induces a lossy mode resonance (LMR), in nanocoated D-shaped optical fibers, the LMRs are induced by several modes. This characteristic allows a quite versatile structure to be obtained, in turn allowing the shape of the LMR to be controlled. By increasing the real part of the refractive index, it was possible to reduce the resonance width up to a value of 24.8 nm (figure of merit 183.1 RIU^{-1}).

Later on, by optimizing the imaginary part of the refractive index, it was possible to increase the figure of merit to 709.4 RIU^{-1}; but several peaks corresponding to the guidance of different modes in the spectrum were visible in the optical spectrum. In order to visualize only one resonance, the width of the nanocoating was reduced to such a point that one single mode was guided. This allowed us to improve the figure of merit to 1021.2 RIU^{-1}. The performance is similar to optimized SPRs, and could be improved with materials of higher refractive index like SnO_2.

In addition, with a pillar nanocoating whose section was nearly square, it was possible to guide only one mode at the same time for both TE and TM polarization, and to obtain a resonance at the same wavelength, which avoids the need for a polarizing system.

The results obtained here should allow more efficient nanocoated D-shaped fiber optical filters, sensors and biosensors to be designed. As an example, it has been analyzed a refractive index sensor for the range 1.3-1.335 with sensitivity 1566 nm/refractive index unit.

Funding

Spanish Ministry of Education and Science-FEDER (TEC2013-43679-R, TEC2016-78047-R); Government of Navarra Health Department (64/2015, 72/2015); Government of Navarra 2016/PI008.